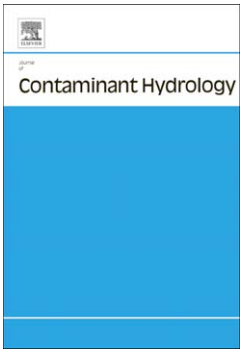

Mixing in confined stratified aquifers

Diogo Bolster, Francisco J. Valdés-Parada, Tanguy LeBorgne, Marco Dentz, Jesus Carrera

PII: S0169-7722(10)00016-1
DOI: doi: 10.1016/j.jconhyd.2010.02.003
Reference: CONHYD 2591

To appear in: *Journal of Contaminant Hydrology*

Received date: 30 October 2009
Revised date: 27 January 2010
Accepted date: 8 February 2010

Please cite this article as: Bolster, Diogo, Valdés-Parada, Francisco J., LeBorgne, Tanguy, Dentz, Marco, Carrera, Jesus, Mixing in confined stratified aquifers, *Journal of Contaminant Hydrology* (2010), doi: 10.1016/j.jconhyd.2010.02.003

Mixing in Confined Stratified Aquifers

Diogo Bolster[a,b], Francisco J. Valdés-Parada[c], Tanguy LeBorgne[d], Marco Dentz[e], Jesus Carrera[e]

[a]*Department of Geotechnical Engineering and Geosciences, Technical University of Catalonia (UPC), 08034 Barcelona, Spain*
[b]*Department of Civil Engineering and Geological Sciences, University of Notre Dame, Indiana, USA*
[c]*División de Ciencias Básicas e Ingeniería, Universidad Autnoma Metropolitana-Iztapalapa, México, D.F., Mexico*
[d]*Geosciences Rennes, UMR 6118, CNRS, Universit de Rennes 1, 3500 Rennes, France*
[e]*Institute of Environmental Assessment and Water Research (IDAEACSIC), 08034 Barcelona, Spain*

Abstract

Spatial variability in a flow field leads to spreading of a tracer plume. The effect of microdispersion is to smooth out concentration gradients that exist in the system. The combined effect of these two phenomena leads to an 'effective' enhanced mixing that can be asymptotically quantified by an effective dispersion coefficient (i.e. Taylor dispersion). Mixing plays a fundamental role in driving chemical reactions. However, at preasymptotic times it is considerably more difficult to accurately quantify these effects by an effective dispersion coefficient as spreading and mixing are not the same (but intricately related). In this work we use a volume averaging approach to calculate the concentration distribution of an inert solute release at preasymptotic times in a stratified formation. Mixing here is characterized by the scalar dissipation rate , which measures the destruction of concentration variance. As such it is an indicator for the degree of mixing of a system. We study preasymptotic solute mixing in terms of explicit analytical expressions for the scalar dissipation rate and numerical random walk simulations. In particular, we divide the concentration field into a mean and deviation component and use dominant balance arguments to write approximate governing equations for each, which we then solve analytically. This allows us to explicitly evaluate the separate contributions to mixing from the mean and the deviation behavior. We find an approximate, but accurate expression (when compared to numerical simulations) to evaluate mixing. Our results

shed some new light on the mechanisms that lead to large scale mixing and allow for a distinction between solute spreading, represented by the mean concentration, and mixing, which comes from both the mean and deviation concentrations, at preasymptotic times.

Keywords: Mixing, Stratified Velocity Fields, Effective Transport

1. Introduction

Transported tracers in a spatially variable velocity field will be subjected to spreading. At the same time, diffusive effects will smooth concentration gradients in the system. The combined effect of these two phenomena leads to an 'effective' enhanced mixing and spreading that can often be asymptotically quantified by an effective dispersion coefficient. Mixing plays an important role in dilution of passive scalars. Beyond this, quantifying mixing accurately plays a fundamental role in chemistry as it often plays a driving role in many chemical reactions (e.g. De Simoni et al., 2005). The aim of this article is to present an analytical approach so as to gain further insight into the total amount of mixing that occurs during early times of transport.

Taylor's seminal work (Taylor, 1953) was the first to quantify this additional dispersive term. He considered the specific case of flow in a circular tube. His concepts can readily be extended to any stratified velocity field in a confined medium and it can be shown that the effective dispersion coefficient has the form $D^{Taylor} = D(1+CPe^2)$. D is the microdispersion coefficient, C is a constant that depends on the specific vertical structure of the flow ($\frac{2}{105}$ for the case of Poiseuille flow) and $Pe = \frac{Ul}{D}$ is the Peclét number. U is the mean flow velocity and l is the width of the flow space. Later, Aris (1956) rigorously quantified this enhanced dispersion in terms of the moments of the plume, relating this dispersive term to the rate of change of the second centered moment with time, thus complementing Taylor's theory. The Taylor-Aris approach to quantify mixing is strictly valid only at late times for which the plume has had sufficient time to sample all the velocities by transverse diffusion. Additionally, its validity is limited to parallel flows. For the case of non-parallel flow there exists a generalized Taylor-dispersion theory for periodic (e.g. Brenner and Edwards, 1993) and stochastic domains (e.g. Lunati et al., 2002). For non parallel flows the behavior of the asymptotic dispersion coefficients is typically more complex (e.g. Gelhar and Axness, 1983; Brenner and Edwards, 1993; Dentz et al., 2002; Dreuzy and Erhel,

2007; Bolster et al., 2009c).

Since Taylor's original paper many works have been dedicated to developing effective theories for preasymptotic times (e.g. Lighthill, 1966; Gill and Sankarasubramanian, 1970; Mercer and Roberts, 1990; Young and Jones, 1991; Camacho, 1993; Latini and Bernoff, 2001; Berentsen et al., 2005). Many of these focus on calculating an apparent dispersion coefficient based on the temporal evolution of the spatial moments of the plume, following the approach of Aris (1956). Such concepts of apparent dispersion coefficients have also been extended to the field of multiphase flows (e.g. Neuweiler et al., 2003; Bolster et al., 2009b). This approach estimates the extent of spreading of the plume, but does not neccesarily quantify mixing. Dentz and Carrera (2007) and Zavala-Sanchez et al. (2009) distinguish two different dispersion coefficients – the apparent and effective dispersion coefficients. The first measures the spread of the plume based on the second centered moment as proposed by many previous researchers; the second measures the second centered moment after centering all the point source plumes associated with a distributed initial condition, thus aiming to quantify mixing. While both are the same at very early and asymptotically late times, during intermediate preasymptotic times the effective coefficient grows more slowly than the apparent one, suggesting that mixing will be over-predicted with an apparent dispersion coefficient.

In this context, by early time we mean earlier than the advective timescale, $\tau_{adv} = l/U$. Similarly, late times refers to any time later than the diffusive time scale $\tau_{diff} = l^2/D$. Note that the Peclét number is the ratio of these two time scales. Intermediate preasymptotic times refers to any time between these two.

In subsurface hydrology spatial variability in the flow field arises due to heterogeneity in the medium. In this work we consider one of the simplest models of heterogeneity, namely a stratified medium where the permeability of the medium varies only in the vertical direction. The resulting flow field is horizontal with variability in the vertical direction only and no flow in the transverse direction. In fluid mechanics this type of flow is referred to as a shear or rectilinear flow (e.g. Kapoor and Anmala, 1998; Young and Jones, 1991). In hydrogeology such stratified velocity models are often used as conceptual models of transport in confined aquifers consisting of layered sedimentary units or for transport in a single fracture (Marle et al. , 1967; Mercado, 1967; Gelhar et al. , 1979; Matheron and de Marsily, 1980; Güven et al., 1984; Dagan, 1990; Cvetkovic and Shapiro, 1989; Fiori and Dagan,

2002; Berentsen and van Kruijsdijk, 2008). The study of transport in stratified flow is in general a valuable way to gain new insights into transport phenomena in heterogeneous media while the simplification of flow stratification allows for a rigorous analytical and numerical treatment.

For randomly stratified velocity fields these questions are approached using stochastic models. Here one aims at the ensemble mean behavior (e.g. Bouchaud et al., 1990; Redner, 1990; Zumofen et al., 1990; Dentz et al., 2008; Fernandez-Garcia et al., 2008), as well as related uncertainties (e.g. Dentz et al., 2009).

In real aquifers, the time it takes to reach the asymptotic dispersion regime, can be very large (of the order of 1000's of years) (Bear (1972)).On the other hand for flow in a fracture such timescales can be on order of seconds or minutes. At pre-asymptotic times, using a Taylor dispersion coefficient can significantly overestimate actual solute spreading and incorrectly calculate mixing (Dentz and Carrera, 2007; Zavala-Sanchez et al., 2009). Therefore, depending on the specific concerns, preasymptotic transport processes should be captured accurately. For example, in a risk analysis where only the maximum extent of a plume is important, a macrodispersion coefficient will provide a worst-case scenario for the extent of a plume. However, if chemical reactions are involved (e.g. Fernandez-Garcia et al., 2008) or the peak concentration is the criterion for risk (e.g. Bolster et al., 2009a), then this is no longer the case and accurate quantification of mixing at preasymptotic times is essential.

At early times mixing is controlled locally by transverse dispersion, which causes sampling of the distribution of vertical velocities and thus leads to spreading. Typically, at early times spreading and mixing are well quantified by the microdispersion coefficient (e.g. Dentz and Carrera, 2007; Fernandez-Garcia et al., 2008). At intermediate times one enters what is often termed a 'superdiffusive' regime where the spreading of a plume is characterized by a dispersion coefficient that grows as $t^{\frac{1}{2}}$ (e.g. Matheron and de Marsily, 1980; Bouchaud and Georges, 1990; Dagan, 1988; LeBorgne et al., 2008a,b). This enhanced spreading leads to increased mixing and the resulting plume is in general non Gaussian.

A good measure of global mixing is the scalar dissipation rate (e.g. Pope, 2000), which is related to the mixing factor (e.g. De Simoni et al., 2005) and the dilution index (Kitanidis, 1994), all defined later in this work. Several studies have aimed to quantify the scalar dissipation rate in heterogeneous flows (e.g. Kapoor and Kitanidis, 1997, 1998; Kapoor and Anmala, 1998).

One of the important features that emerges from all these studies is that it is not sufficient to only quantify the vertically averaged concentration, which is sufficient for breakthrough curve prediction. In order to quantify mixing correctly one must take into account higher concentration moments. Battiato et al. (2009) showed that commonly used upscaling approaches can fail to accurately predict mixing and chemical reactions, because they do not properly quantify such local scale mixing effects as they disregard local concentration correlations.

Herein, we present an approximate preasymptotic theory to quantify mixing in stratified velocity fields. We follow the works of Valdés-Parada et al. (2009) and Porter et al. (2008) to derive approximate equations for the mean concentration and the concentration deviations. A dominant balance argument for the deviation concentration equation allows us to obtain an approximate solution for its field. Feeding this solution back into the equation for the mean concentration and performing another dominant balance approximation allows us to solve this equation. The mean concentration provides an idea of the extent of the plume (i.e. spreading), while the concentration deviations allow one to properly quantify local concentration gradients and thus mixing. We then illustrate the theory by applying it to two cases: (i) Poiseuille flow, which is an example of an analytical shear velocity field (i.e. vertically stratified velocity) and (ii) a sample vertical stratified field representative of a geological formation. The analytical results are compared to the results of numerical simulations for validation purposes.

The paper is structured as follows: in Section 2 we present the upscaled model along with the measures we use to quantify mixing in Section 3; in Section 4 we present examples for specific cases where we compare the analytical results with those of numerical random walk simulations and we wrap up the paper with conclusions and discussion in Section 5.

2. Model - Analytical Approximation of Concentrations

Here we study the transport of a conservative tracer in a two-dimensional confined vertically stratified velocity field $u_i(x, y) = \delta_{ix} u(y)$, $i = x, y$. The transport in such a flow field is governed by the advection diffusion equation

$$\frac{\partial c(x,y,t)}{\partial t} + u(y)\frac{\partial c(x,y,t)}{\partial x} = D\frac{\partial^2 c(x,y,t)}{\partial x^2} + D\frac{\partial^2 c(x,y,t)}{\partial y^2} \qquad (1)$$

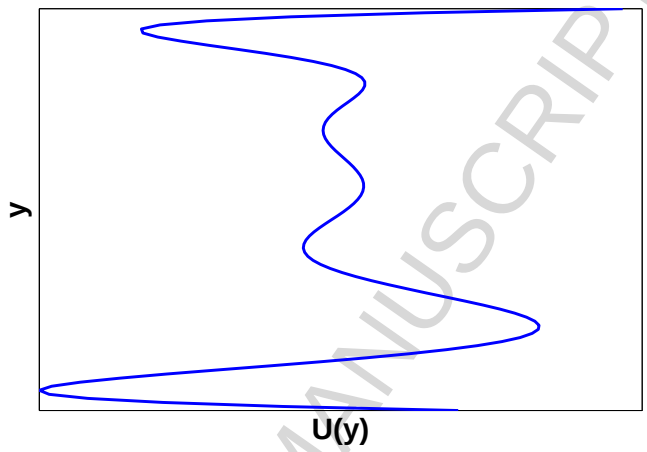

Figure 1: A sample shear/stratified flow where the horizontal velocity varies in the transverse direction.

subject to the boundary conditions

$$\left.\frac{\partial c}{\partial y}\right|_{y=0,l} = 0, \qquad c|_{x=\pm\infty} = 0 \tag{2}$$

where l is the transverse width of the transport domain. The initial condition is given by

$$c(x, y, t = 0) = f(x, y). \tag{3}$$

$c(x, y, t)$ is the local concentration.

2.1. Nondimensionalisation

We now introduce the following dimensionless quantities

$$\hat{x} = \frac{x}{l}, \qquad \hat{y} = \frac{y}{l}, \qquad \hat{c} = \frac{c}{c_{ref}}, \qquad \hat{t} = \frac{t}{\tau_d}, \qquad \hat{u} = \frac{ul}{D}, \tag{4}$$

where c_{ref} is a reference concentration value. Here we choose the diffusive time scale $\tau_D = l^2/D$ as the characteristic time with which we nondimensionalize time. This is because it is transverse diffusive effects that ultimately

cause the system to achieve its asymptotic state. Introducing these quantities into (1) results in the following dimensionless governing equation

$$\frac{\partial \hat{c}(\hat{x},\hat{y},\hat{t})}{\partial \hat{t}} + \hat{u}(\hat{y})\frac{\partial \hat{c}(\hat{x},\hat{y},\hat{t})}{\partial \hat{x}} = \frac{\partial^2 \hat{c}(\hat{x},\hat{y},\hat{t})}{\partial \hat{x}^2} + \frac{\partial^2 \hat{c}(\hat{x},\hat{y},\hat{t})}{\partial \hat{y}^2} \tag{5}$$

with the boundary conditions

$$\left.\frac{\partial \hat{c}}{\partial \hat{y}}\right|_{\hat{y}=0,1} = 0, \qquad \hat{c}|_{\hat{x}=\pm\infty} = 0 \tag{6}$$

and the initial condition

$$\hat{c}(\hat{x},\hat{y},\hat{t}=0) = \hat{F}(\hat{x},\hat{y}). \tag{7}$$

For simplicity of notation, in the following, we will drop the hats. and understand that all quantities under consideration are non-dimensional according to (4).

2.2. Cross-Sectional Averaging

The objective here is to develop an effective transport description that is less complex than the original problem but retains its salient features. Following Taylor (1953), we average vertically, which leads to an effective one-dimensional transport description.

To this end, we define the cross-sectional averaging operator

$$\langle\psi\rangle = \int_0^1 \psi dY, \tag{8}$$

in which, ψ denotes any quantity in the system, such as the velocity or the tracer concentration. We decompose ψ into its average $\langle\psi\rangle$ and deviations $\widetilde{\psi}$ about it,

$$\psi = \langle\psi\rangle + \widetilde{\psi}. \tag{9}$$

Average quantities are denoted by angular brackets, while the deviation quantities are denoted by a tilde. By definition, the average of the deviations is zero

$$\langle\widetilde{\psi}\rangle = 0. \tag{10}$$

With these definitions we decompose the velocity and concentration fields into average and deviations

$$u(y) = Pe + \widetilde{u}(y), \qquad c(x,y,t) = \langle c\rangle(x,t) + \widetilde{c}(x,y,t). \tag{11}$$

The average velocity in this framework is given by the Peclét number $Pe = l\langle u\rangle/D$, which is a measure of the influence of advective relative to diffusive transport processes.

We expand the velocity perturbations $\widetilde{u}(y)$ as a Fourier series

$$\widetilde{u}(y) = \sum_{n=1}^{\infty} a_n \cos\left(n\pi y\right) \qquad a_n = 2\int_0^1 \widetilde{u}(\xi)\cos\left(n\pi\xi\right)\mathrm{d}\xi. \tag{12}$$

In order to obtain explicit expressions for the average concentration $\langle c\rangle$ and its deviations $\widetilde{c}$ we resort to the approach of Valdés-Parada et al. (2009), who derived a closed system of approximate equations for the mean concentration $\langle c\rangle$ and its deviations $\widetilde{c}$ in a circular tube. In this approach, one neglects the local and nonlocal advective contribution to the deviation concentration $\widetilde{c}$ and localizes the source from the mean concentration. The details of these approximations are outlined in Appendix A. The approximate governing equation for the mean concentration is

$$\frac{\partial\langle c\rangle}{\partial t} + Pe\frac{\partial\langle c\rangle}{\partial x} = D^a(t)\frac{\partial^2\langle c\rangle}{\partial x^2} + \phi(x,t) \tag{13}$$

where $D^a(t)$ is the time dependent Taylor dispersion coefficient

$$D^a(t) = 1 + \sum_{n=1}^{\infty}\frac{a_n^2}{\pi^2 n^2}\left[1 - e^{-n^2\pi^2 t}\right], \tag{14}$$

and $\phi(x,t)$ a source function defined by (A.18) in Appendix A. The initial-boundary conditions for $\langle c\rangle$ are given by

$$\langle c\rangle(x, t=0) = \langle F\rangle(x), \qquad \lim_{x\to\pm\infty}\langle c\rangle(x,t) = 0. \tag{15}$$

The concentration deviations are obtained by subtracting the averaged transport equation from the original one, which can be approximated by (see appendix A for details)

$$\frac{\partial\widetilde{c}}{\partial t} - \left(\frac{\partial^2\widetilde{c}}{\partial x^2} + \frac{\partial^2\widetilde{c}}{\partial y^2}\right) = -\widetilde{u}(y)\frac{\partial\langle c\rangle}{\partial x} \tag{16}$$

with the boundary conditions

$$\widetilde{c}|_{x=\pm\infty} = 0, \qquad \left.\frac{\partial \widetilde{c}}{\partial y}\right|_{y=0,1} = 0, \tag{17a}$$

and the initial condition

$$\widetilde{c}(x, y, t = 0) = \widetilde{F}(x, y). \tag{17b}$$

Equation (16) is valid under the constraint given in (A.6), which is a length-scale constraint. Equations (15) and (16) point out that concentration deviations are driven by the initial condition (17 (b)) and by the convective displacement fluctuations (rhs of (16)). These fluctuations are dissipated by microscale mixing the x and y directions. Explicit solutions for $\langle c\rangle$ and $\widetilde{c}$ can be obtained straightforwardly in terms of the respective Green's functions. Thus, the mean concentration can be written as

$$\langle c\rangle(x, t) = d_0(x, t) + d_1(x, t) \tag{18}$$

where $d_0(x, t)$ and $d_1(x, t)$ are given by (A.19) and (A.20) in Appendix A. The term $d_0(x, t)$ is due to the initial conditions, $d_1(x, t)$ due to the source term.

For the concentration deviations one obtains an expression that is spatially non-local in the gradient of the mean concentration. Localizing it (Appendix A) yields

$$\widetilde{c}(x, y, t) = b_0(x, y, t) + b_1(y, t)\frac{\partial\langle c\rangle(x, t)}{\partial x}, \tag{19}$$

where $b_0(x, t)$ and $b_1(y, t)$ are given by (A.14) and (A.15) in Appendix A. Again, the first term reflects the boundary condition, the second the source term in (16).

3. Quantifying Mixing - Analytical Expressions

Mixing is produced by the interaction of concentration gradients and diffusion. In this context, the following expression has been identified as a local mixing measure (in dimensionless terms),

$$m(x, y, t) = \left[\frac{\partial c(x, y, t)}{\partial x}\right]^2 + \left[\frac{\partial c(x, y, t)}{\partial y}\right]^2. \tag{20}$$

This term appears in the expression for the reaction rates of mixing driven chemical reactions (e.g. De Simoni et al., 2005) as well as in the expression for the dilution index as defined by Kitanidis (1994). The same expression in terms of the gradients of the concentration deviations appears in the evolution equation for the concentration variance (e.g. Kapoor and Gelhar, 1994a,b; Kapoor and Kitanidis, 1998). Its average has been studied as 'fluctuation dissipation function' in, e.g., Kapoor and Gelhar (1994a).

In the following we focus on the space integral of the mixing factor (20)

$$\chi(t) = \int_\Omega m(x,y,t) d\Omega, \tag{21}$$

as a global mixing measure. We defined here the integral over the entire spatial domain as

$$\int_\Omega d\Omega = \int_0^1 \int_{-\infty}^{\infty} dx dy. \tag{22}$$

Expression (21) has been known in the literature as scalar dissipation rate (e.g. Pope, 2000). Multiplying (5) by $c(x,y,t)$, integrating over the whole spatial domain and applying the divergence theorem one can readily show that

$$\chi(t) = -\frac{dM(t)}{dt}. \tag{23}$$

where we defined the concentration moment

$$M(t) = \int_\Omega c(x,y,t)^2 d\Omega. \tag{24}$$

What (23) illustrates is that in order to correctly understand mixing it is not sufficient to have a measure of the average of the concentration, but rather the average of the square of the concentration. Using the decomposition (11) for the concentration in (23), we obtain

$$M(t) = M_1(t) + M_2(t), \tag{25}$$

where $M_1(t)$ and $M_2(t)$ are the contributions due to the mean concentration and the concentration deviations, respectively. They are given by

$$M_1(t) = \int_\Omega \langle c \rangle (x,t)^2 d\Omega, \qquad M_2(t) = \int_\Omega \widetilde{c}(x,y,t)^2 d\Omega. \tag{26}$$

When the concentration deviations are much smaller than the average concentrations, one expects the one-dimensional average concentration field to accurately represent mixing as well as spreading. However, at preasymptotic times, where the deviation concentrations are not small relative to the average only accounting for the average concentration will not correctly quantify mixing. The effective modeling approach presented in the previous section provides a method to quantify solute mixing in this preasymptotic regime as it gives explicit (approximate) expressions for the mean concentration and, more importantly, for the concentration deviations. Inserting (18) and (19) into (26) gives the approximate expressions for $M_1(t)$ and $M_2(t)$

$$M_1(t) = \int_\Omega d_0(x,t)^2 d\Omega + \int_\Omega 2d_0(x,t)d_1(x,t)d\Omega + \int_\Omega d_1(x,t)^2 d\Omega \tag{27}$$

$$M_2(t) = \int_\Omega b_0(x,y,t)^2 d\Omega + \int_\Omega 2b_0(x,y,t)b_1(y,t)\frac{\partial\langle c\rangle(x,t)}{\partial x}d\Omega + \int_\Omega b_1(y,t)^2\left[\frac{\partial\langle c\rangle(x,t)}{\partial x}\right]^2 d\Omega. \tag{28}$$

In the following we study the global mixing rate $\chi(t)$ and its quantification using the effective expressions (27) and (28). To this end, we perform numerical random walk particle tracking simulations of the direct problem (see Appendix B) and compare the outcome for the global mixing rate to the approximate upscaled expressions (27) and (28).

4. Application to Specific Stratified Flows

Here we study the global mixing rate for two commonly studied initial conditions, namely a line and point source. We consider 4 different velocity fields. These are depicted in Figure 2 and are described by

(a) Poiseuille flow, which represents pressure driven flow between two flat plates.

(b) 250 layers of thickness 4×10^{-3} each with a random velocity, chosen from a lognormal distribution of mean 100 (the Péclet number for all cases presented herein) and relative variance 1/2.

(c) Same as (b) but with a variance 1.

(d) Same as (b) but with a variance 4.

While case (a) is not a likely flow in stratified geological media it satisfies the requirement of having no transverse flow and a horizontal flow that

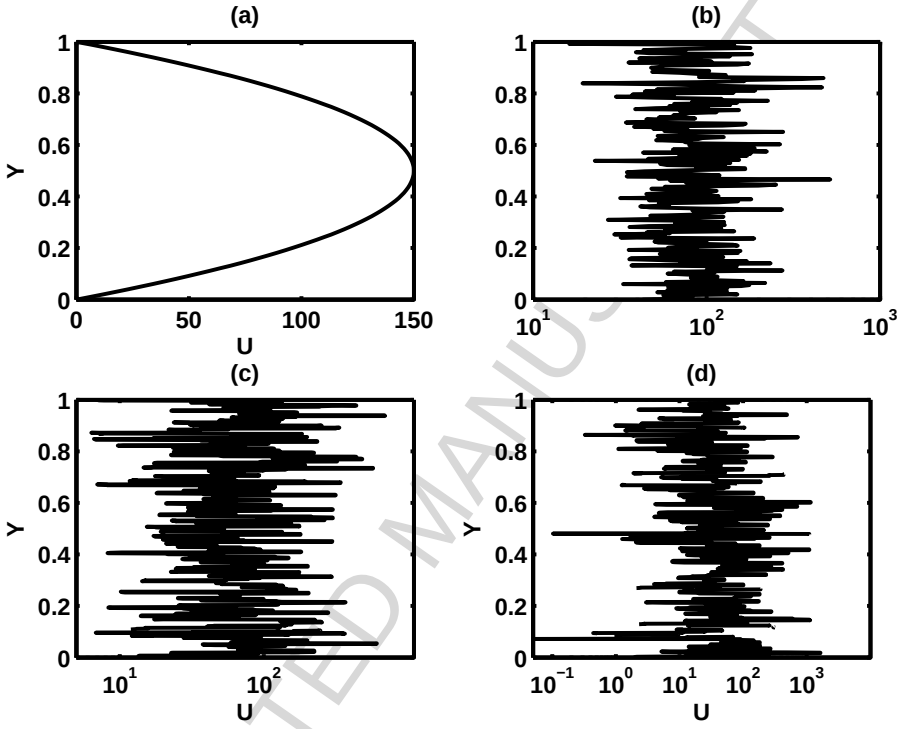

Figure 2: The four velocity distributions (a)-(d) considered in this work. Note the horizontal scales for fields (b)-(d).

varies only in the transverse direction. Additionally it is likely to happen in geological media, but at the scale of fractures or pores. It has a simple form that is conducive to analytical solutions and has also been studied extensively in the literature, thus making it easy to compare to previous cases. The velocity fields in cases (b)-(d) are divergence-free solutions of the Darcy equation for stratified porous media characterized by lognormal distributions of the hydraulic conductivity. They reflect more typically studied cases each with an increasing degree of heterogeneity (note in Figure 2 how they progressively span more orders of magnitude of velocity). In all cases presented here the Péclet number considered is $Pe = 10^2$, although both larger and smaller values were also studied with similar results.

4.1. Line Source

The first example we consider is that of the line source initial condition, namely

$$c(x, y, t = t_0) = \delta(x - x_0) \tag{29}$$

where $\delta(x)$ is the Dirac delta distribution. In terms of average and deviation concentrations this means that the initial conditions are

$$\langle c \rangle(x, t = t_0) = \delta(x - x_0), \qquad \widetilde{c}(x, y, t = t_0) = 0 \tag{30}$$

which in turn means that

$$b_0(x, y, t) = 0, \qquad b_1(y, t) = \sum_{n=1}^{\infty} \frac{a_n}{n^2\pi^2} \cos\left(n\pi y\right)\left(1 - e^{-n^2\pi^2 t}\right), \quad \phi(x, y, t) = 0. \tag{31}$$

As such, there is no source term in equation (13) for the average concentration and the solution depends only on the initial condition. It is given by

$$\langle c \rangle(x, t) = \frac{\exp\left\{-\frac{[x - Pe(t-t_0)]^2}{2\kappa^a(t|t_0)}\right\}}{\sqrt{2\pi\kappa^a(t|t_0)}}, \qquad \kappa^a(t|t_0) = 2\int_{t_0}^{t} D^a(\tau)\mathrm{d}\tau. \tag{32}$$

In the following we set the initial time $t_0 = 0$ and set $\kappa^a(t|0) \equiv \kappa^a(t)$. From the average concentration, we can compute the fluctuating component using (19).

$$\widetilde{c}(x, y, t) = -b_1(y, t)\frac{(x - Pet)}{\sqrt{2\pi\kappa^a(t)^3}} \exp\left[-\frac{(x - Pet)^2}{2\kappa^a(t)}\right]. \tag{33}$$

Sample plots of the concentration field calculated with the analytical solution for Poiseuille flow at different times are shown in Figure 3. Corresponding particle distributions from random walk simulations at various times are shown in Figure 4, which allow for a qualitative comparison of the solutions for the particle distributions. A quantative comparison of the concentration distribution is not pursued here (see Valdés-Parada et al. (2009) for one). At early times the plume is fairly close to a one dimensional plume with some bending due to the velocity field. At late times the plume returns to looking fairly one-dimensional. However at intermediate times the two-dimensional structure of the plume is evident. Due to the approximate nature of the solution, the concentration field from the simulations and analytical solution

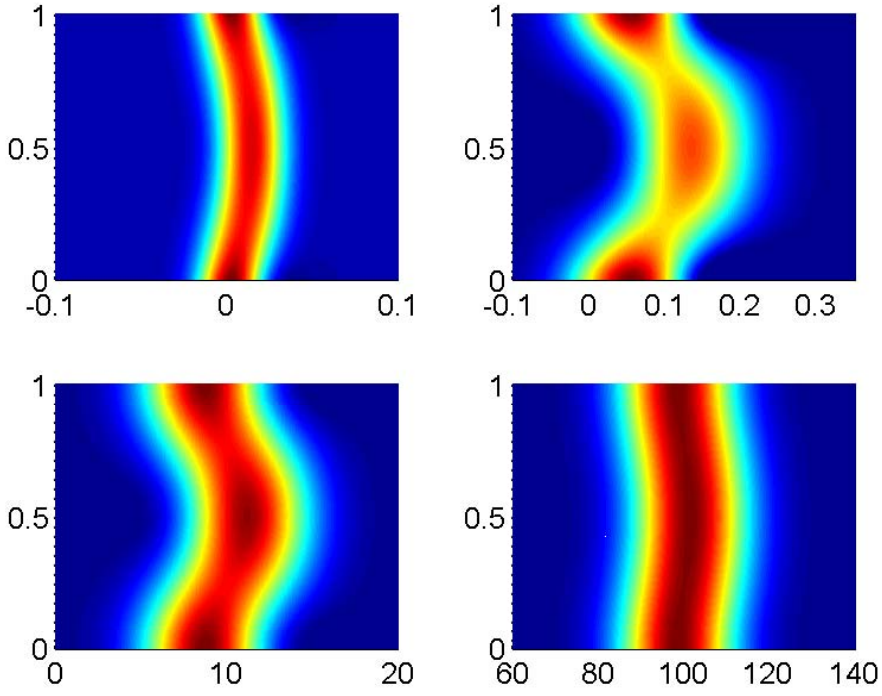

Figure 3: Concentration for the line source initial condition in Poiseuille flow at various times. $t = 10^{-4}$ (top left), $t = 10^{-3}$ (top right), $t = 10^{-1}$ (bottom left), $t = 1$ (bottom right).

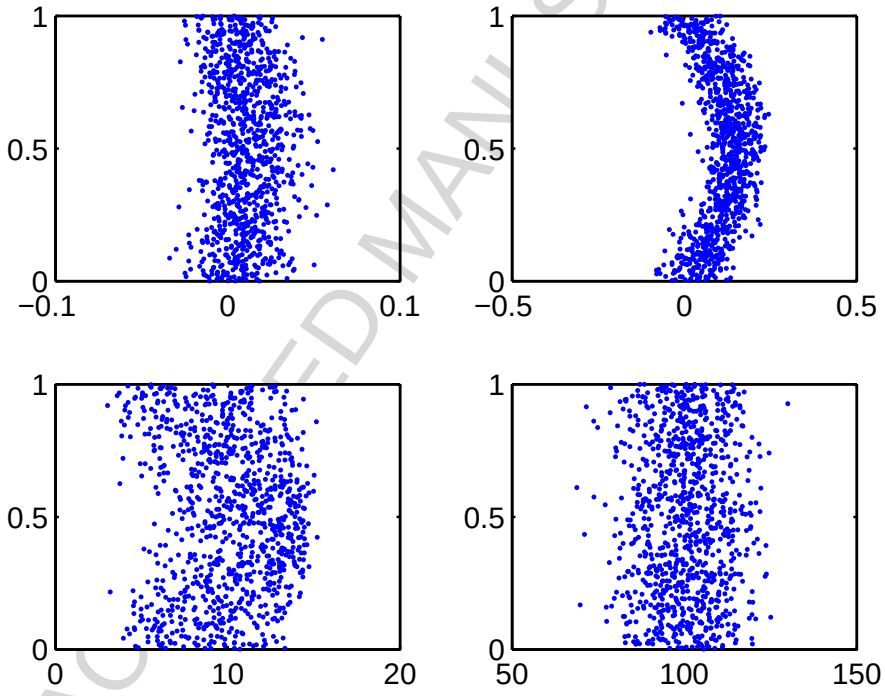

Figure 4: Plumes from random walk simulations for the line source initial condition in Poiseuille flow at various times. $t = 10^{-4}$ (top left), $t = 10^{-3}$ (top right), $t = 10^{-1}$ (bottom left), $t = 1$ (bottom right). $Pe = 100$

are qualitatively slightly different. The approximate effective model will not predict the precise shape of the concentration distribution. However, this was not the aim of an effective model. We are after an effective description of the mean concentration and the mixing behavior as quantified by the global mixing rate. Valdés-Parada et al. (2009) show that the effective description works quite well at predicting average concentration breakthrough curves. It is still an open question whether the same can be said for mixing, which requires knowledge of the concentration deviation. In order to study this, we first consider the contributions $M_1(t)$ and $M_2(t)$ separately. They are obtained by substituting (32) and (33) into (26), which leads to

$$M_1(t) = \frac{1}{\sqrt{4\pi\kappa^a(t)}} \tag{34}$$

and

$$M_2(t) = \frac{1}{\sqrt{16\pi\kappa^a(t)^3}} \sum_{n=1}^{n=\infty} \frac{a_n^2}{2n^4\pi^4} \left(1 - e^{-n^2\pi^2 t}\right)^2 \tag{35}$$

Now we can evaluate the amount of mixing taking place in our domain. Both $M_1(t)$ and $M_2(t)$ depend heavily on the structure of the flow, which is captured by the Fourier coefficients a_n. The appearance of the $\frac{1}{n^4}$ and $e^{-n^2\pi^2 T}$ terms suggests that flow with long wave lengths (contributing to small n in a_n coefficients) have a great degree of influence on mixing. The plots in figure 5 depict $M_1(t)$, $M_2(t)$ and their sum $M(t)$, (25), and the values calculated from numerical simulations. At early times the system is entirely dominated by the average concentration and the contributions from the perturbation concentrations are several orders of magnitude smaller. This is because very little spreading of the line initial condition takes place at early time and so concentration is well represented by a Gaussian whose thickness is determined by the diffusion coefficient. This means that the average and actual concentrations are fairly close in value. This is similar to what has been previously observed by Dentz and Carrera (2007). At these early times the system behaves as a one dimensional systems as reflected by the $t^{-1/2}$ decay of $M(t)$ at early times. As time advances, spreading effects kick in and cause the width of the plume to grow superdiffusively as noted by the change of slope of the average concentration squared line.

At these intermediate times, the influence of the perturbation concentration, while still smaller than the average concentration is no longer negligible

and contributes to the total value. This is the region where the average value $M_1(t)$ (blue line) does not coincide with the numerically calculated value (dots). However, the difference between the numerical and average concentrations appears to be well represented by $M_2(t)$, suggesting that the analytical solution does a good job of calculating the actual mixing that will occur.

Of particular interest, but perhaps unsurprising, should be that the difference between the mean square concentration and the concentration fluctuation at intermediate times increases progressively for flow fields (b) through (d) reflecting the greater degree of heterogeneity. Larger degrees of heterogeneity cause greater spreading, hence greater deviations from mean behavior. Interestingly case (a) presents the largest difference. This is a reflection of the long wave length nature of this flow relative to others, meaning that the low Fourier wavelengths (quantified by a_n) have a lot of weight and contribute more significantly to the deviation term $M_2(t)$ in (35). Physically this reflects the greater degree of spreading induced by the longer wavelengths that in turn influences mixing.

One of the questions that arises is whether spreading is over predicted or under predicted by only considering the mean case that is determined solely by $D^a(t)$. It is often argued that $D^a(t)$ over predicts mixing during preasymptotic times as $D^a(t)$ suggests a wide one-dimensional Gaussian plume with peak concentrations that are lower than actual peak concentration which would be better measured by an effective dispersion coefficient (e.g. Dentz and Carrera, 2007). However, if we look at the behavior of $M_2(t)$ it quickly emerges that this is not entirely true. At early times this is an increasing function. However at a certain point in time it turns and begins to decrease as shown in Figure 6 . As mixing/scalar dissipation depends on the slope of $M(t)$ it is clear that at early times this slope will be larger than that predicted solely by the average concentration, which implies less actual mixing. However, when $M_2(t)$ begins to decrease with time this indicates that more mixing occurs than would be predicted by the average concentration alone, reflecting the two dimensional nature of the plume that has been created by spreading effects, thus increasing mixing by transverse diffusion. It should also be noted that the differences at early times on mixing are negligible and, as stated by Dentz and Carrera (2007), only become comparable when spreading effects kick in (i.e. for times greater than the advection time scale) and at these times mixing is over predicted.

At later 'asymptotic' times, the perturbation term dies away and returns

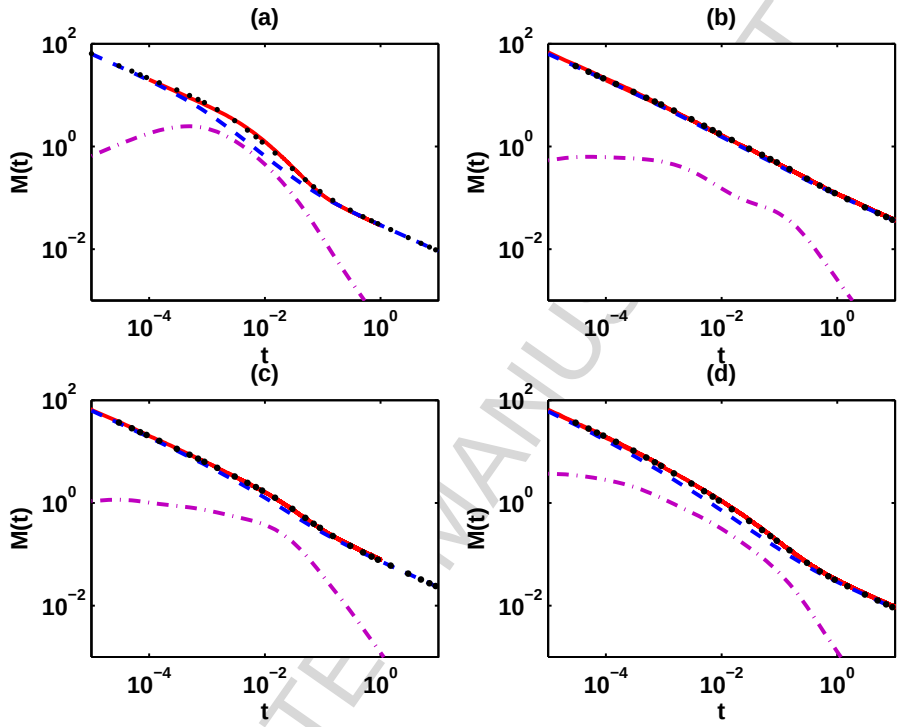

Figure 5: $M(t)$ (black $\cdot$) against time for line source initial condition for cases (a)-(d). $M_1(t)$ (dark blue - -), $M_2(t)$ (purple - $\cdot$) and numerical Simulations (red -). Note that the numerical and effective $M(t)$ virtually coincide in all four cases.

to being several orders of magnitude smaller than the average term, suggesting again that at asymptotic times mixing, as well as spreading, are well characterized by the average concentration and apparent dispersion coefficient. It is a commonly held belief that at these asymptotic times mixing and spreading are the same. Here we illustrate that, at least to leading order, this is definitely true as at late times $M_1(t) \gg M_2(t)$. Recall that $M_1(t)$, the contribution from the mean concentration, reflects spreading.

With these results we can calculate the global mixing rate $\chi(t)$, which is given by time derivation of the sum of (34) and (35),

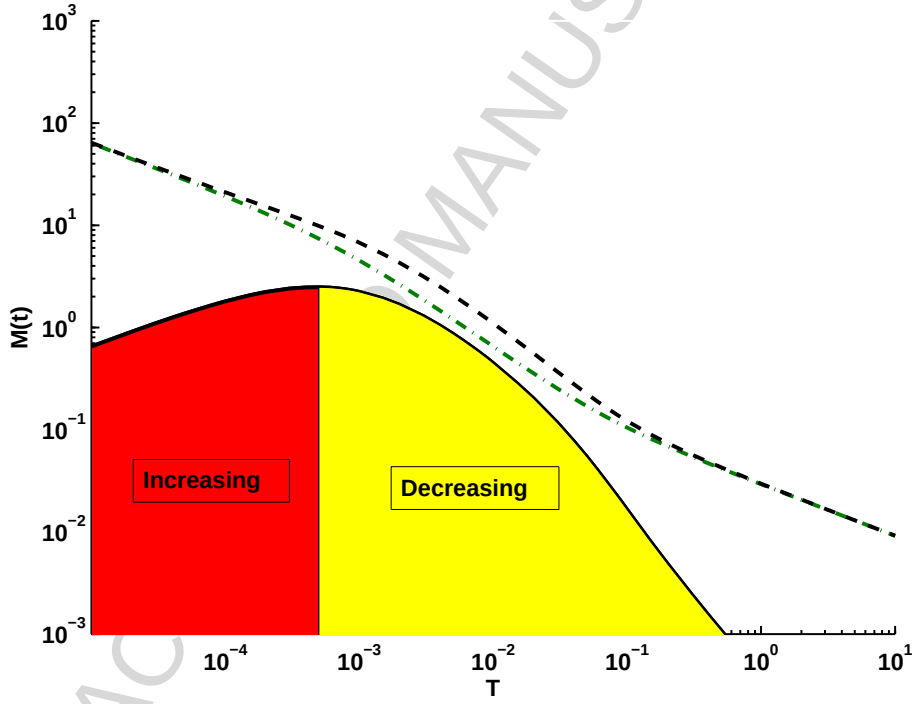

Figure 6: $M(t)$ (black - -) against time for Poiseuille flow and line source initial condition. $M_1(t)$ (green - .), $M_2(t)$ (black -). The red highlighted region indicates where $M_2(t)$ is increasing, while the yellow region marks where this quantity is decreasing.

$$\chi(t) = \frac{1}{\sqrt{\pi\kappa^a(t)^3}} D^a(t) - \frac{3}{2\sqrt{4\pi\kappa^a(t)^5}} D^a(t) \sum_{n=1}^{\infty} \frac{a_n^2}{2n^4\pi^4} \left(1 - e^{-n^2\pi^2 t}\right)^2 + \frac{1}{2\sqrt{16\pi\kappa^a(t)^3}} D^a(t) \sum_{n=1}^{\infty} \frac{a_n^2}{n^2\pi^2} \left(1 - e^{-n^2\pi^2 T}\right) \quad (36)$$

where the first term comes from the contribution of $M_1(t)$ and the second term from $M_2(t)$.

A plot of $\chi(t)$ for the Poiseuille flow case is shown in Figure 7. In this figure we identify the advective and diffusive time scales by vertical lines. Note that, at times earlier than the advective time, the scalar dissipation is faithfully represented by the mean behavior only. This is also the case at times later than the diffusive time scale. However, at intermediate times, the contribution due to the deviation concentration is of comparable order to the mean and neglecting the deviation behavior can result in underestimating χ by close to an order of magnitude.

4.2. Point Source

Here we consider the initial condition of a point source, i.e.

$$c(x, y, t = 0) = \delta(x - x_0)\delta(y - y_0), \quad (37)$$

which in terms of average and perturbation concentration means

$$\langle c \rangle(x, t = 0) = \delta(x - x_0), \quad (38)$$

$$\widetilde{c}(x, y, t = 0) = \delta(x - x_0)\left[\delta(y - y_0) - 1\right]. \quad (39)$$

Figure 8 illustrates how a point source plume released from $y_0 = 0.5$ evolves over time in Poiseuille flow. At early times (Figure 8 (a)) the plume behaves much like a point sources in uniform flow. At intermediate times (Figure 8 (b)) the plume diffuses laterally and is distorted by spreading due to vertical gradients in the velocity field. At later times, once the plume has sampled the vertical cross section (Figure 8 (c), (d)) the plume looks almost indistinguishable from the line source case in figure 4 reflecting the fact that due to diffusive smearing the system is "forgetting" its initial condition.

We set without loss of generality $x_0 = 0$. Given this initial condition and using (A.14) we derive

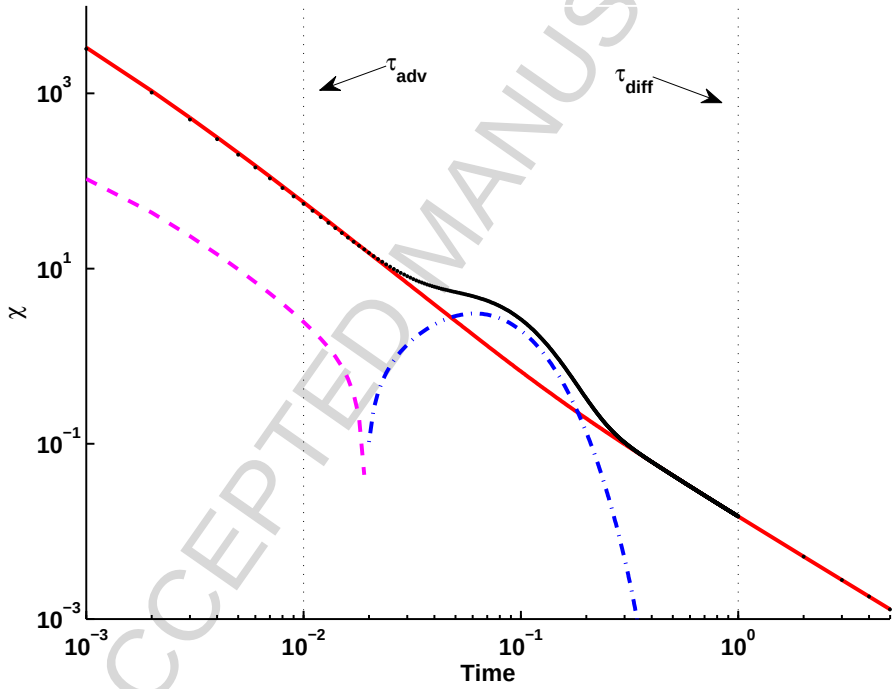

Figure 7: The global mixing rate $\chi(t)$ in (36) against time for the line source initial condition in Poiseuille flow. The red solid line is if we only consider the average concentration. The black dots are for the total scalar dissipation rate. The other two lines correspond to the deviation concentration effects. Dark blue indicates a positive contribution, while the dashed purple line is actually a negative value

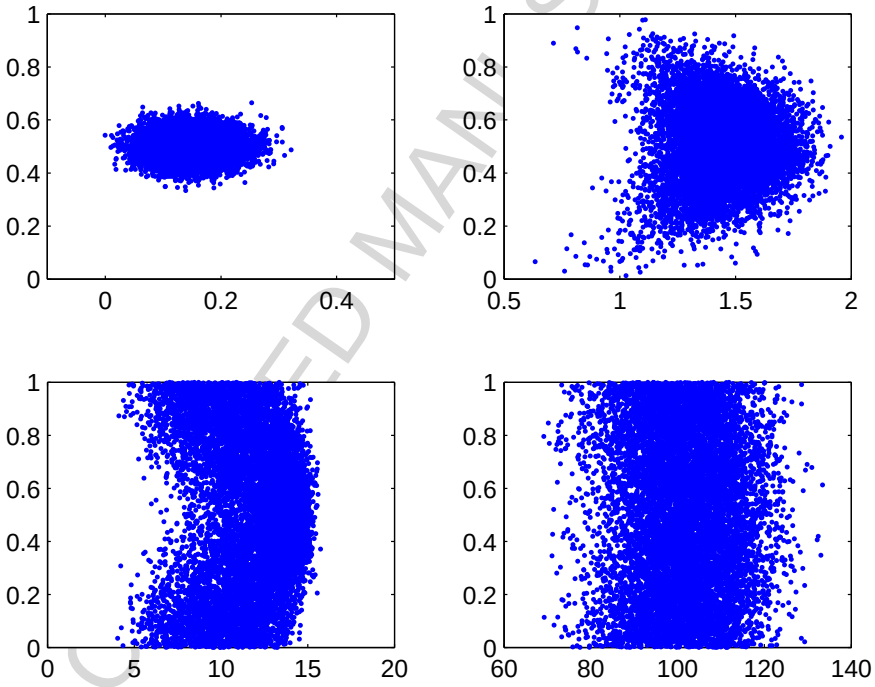

Figure 8: Plumes from random walk simulations for the point source initial condition in Poiseuille flow at various times. $t = 10^{-3}$ (top left), $t = 10^{-2}$ (top right), $t = 10^{-1}$ (bottom left), $t = 10^{0}$ (bottom right). The plots are for the case $Pe = 100$

$$b_0(x,t) = \frac{1}{\sqrt{4\pi t}} e^{-\frac{(x-Pet)^2}{4t}} 2 \sum_{n=1}^{\infty} \cos(n\pi y) \cos(n\pi y_0) e^{-n^2\pi^2 t}. \tag{40}$$

With (40) and (A.18) we can also calculate the source term $\phi(x,t)$ in (14) as

$$\phi(x,t) = \frac{-(x-Pet)}{2\sqrt{4\pi t^3}} e^{\frac{-(x-Pet)^2}{4t}} \sum_{n=1}^{\infty} a_n \cos(n\pi y_0) e^{-n^2\pi^2 t} \tag{41}$$

Finally, using (18) we then obtain for the mean concentration the integral expresion

$$\begin{aligned} \langle c \rangle(x,t) &= \langle c_0 \rangle(x,t) - (x-Pet) \int_0^t \sum_{n=1}^{\infty} a_n \cos(n\pi y_0) e^{-n^2\pi^2\tau} \\ &\quad \times \frac{e^{\frac{-(x-Pet)^2}{2[\kappa^a(t|\tau)+2\tau]}}}{\sqrt{2\pi[\kappa^a(t|\tau)+2\tau]^3}} \mathrm{d}\tau \end{aligned} \tag{42}$$

where $\langle c_0 \rangle(X,T)$ is the solution from the previous section on the line source initial condition. Unfortunately, we are unable to find an analytical manner in which to execute the final integral over τ and as such are forced to solve this by numerical quadrature.

The solution for the concentration deviations $\widetilde{c}(x,y,t)$ is given by (19), where $b_0(x,y,t)$ is given in (40) and $b_1(y,t)$ is the same as for the line source, given in (31) .

Comparisons of numerical simulations and theoretical results for $M(t)$ over time in all four flow fields are shown in Figure 10. Once again the agreement between theory and simulations is evident, although there is some subtle disagreement for case (d) at intermediate times. This disagreement though is still quite small and is unsurprising as the approximations in the analytical solution may become questionable for cases where the variations in velocity are as large as they are in case (d). None the less it appears that the dominant balances invoked in Appendix A are still valid for these stratified fields, which suggests that the contribution to mixing from the nonlocal convective term in the governing equation for $\widetilde{c}$ (A.2) is still sub dominant or balanced by the local convection term. The most important

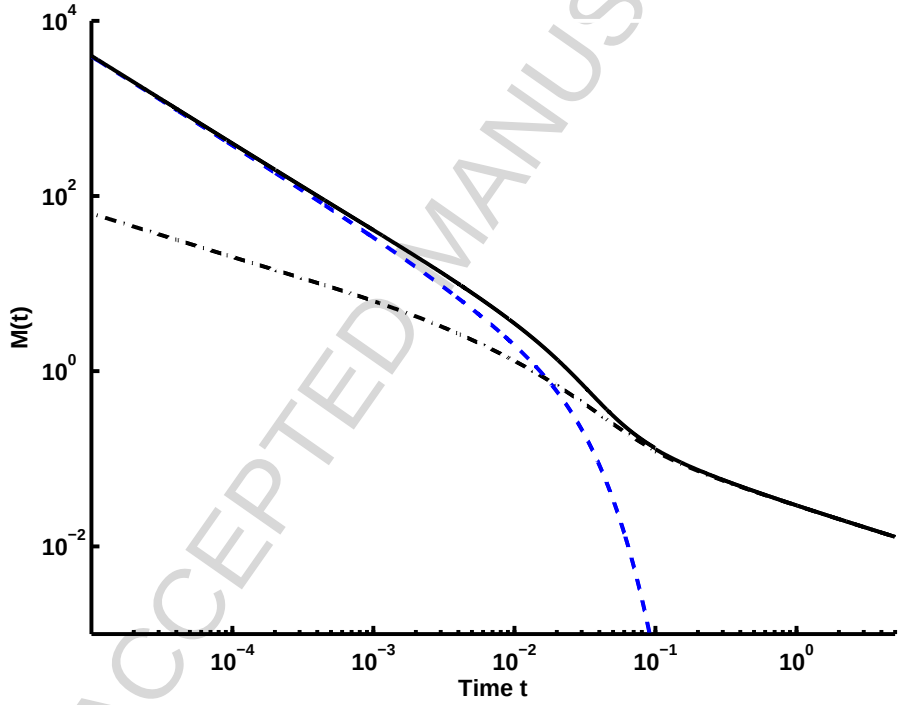

Figure 9: $M(t)$ for point source for the Poiseuille flow example . The contribution due to the mean concentration $\langle c \rangle$, $M_1(t)$ is given by the black dash-dot line; the contribution from the deviation concentration $\widetilde{c}$, $M_2(t)$ is given by the blue dashed line and the solid black line represents the sum of these two.

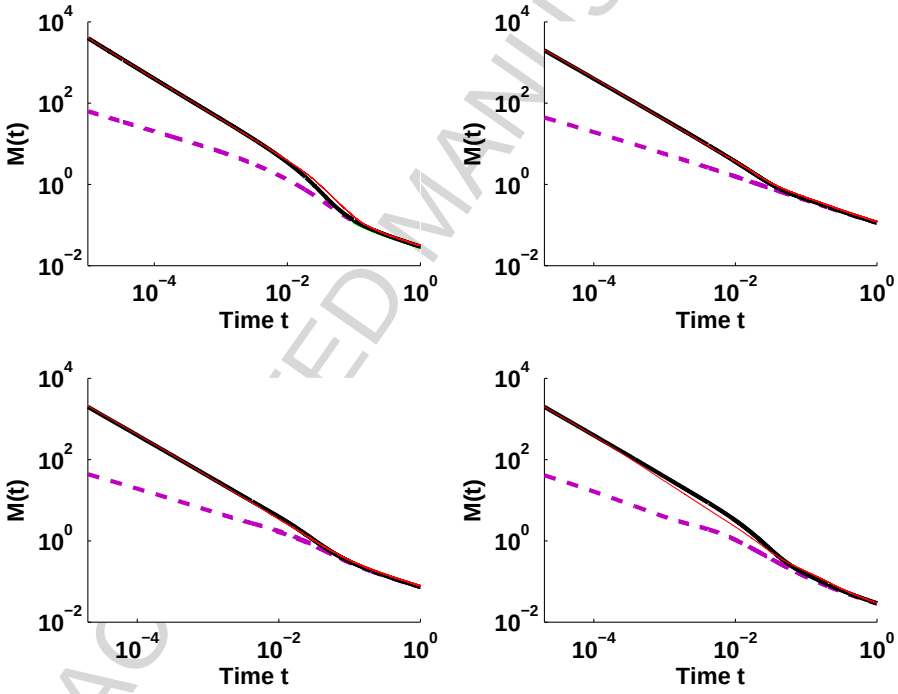

Figure 10: $M(t)$ (thick black -) for cases (a)-(d) compared with numerical simulations. $M_1(t)$ (purple - -) and numerical results (thin red -).

feature though is that, unlike the line source case, at early times the average concentration solution is absolutely incapable of reproducing the behavior observed in the simulations. This also is unsurprising as at early times the entire notion of what an average concentration represents is questionable as the averaging will smear out all strong local effects, which for the case of a point source clearly dominate. At later times the averaging works because diffusion has in fact done its best to smear out local vertical gradients. Once again it is evident that knowledge of an average concentration, while adequate for predicting breakthrough curves or the likes, is simply not sufficient to quantify mixing. A correct quantification of mixing requires knowledge of the average value of the concentration squared.

Figure 9 reveals the detailed structure of $M(t)$ for a point source released at $y_0 = 0.5$ for flow field (a). At early times it is completely dominated by its purely diffusive two-dimensional behavior.

At intermediate times spreading effects from the average concentration begin to contribute to the total value. Ultimately at late times the average contribution dominates completely in the same manner as for the line source.

Figure 11 displays the scalar dissipation rate $\chi(t)$ for the point source in flow field (a). Cases (b)- (d) behave similarly. In Figure 11 two contributions are shown, namely the contribution from the mean concentration field and the contribution from the deviation concentration field. At early times (less than $t = 10^{-2}$) the deviation contribution dominates entirely and is several orders of magnitude larger than the mean contribution, thus again reflecting the two dimensional nature of the plume and the lack of proper meaning of a mean concentration at early times. For times more or less between $10^{-2} < t < 10^{-1}$ both the mean and the deviation contribution are of similar order of magnitude. Ultimately, at time $t > 10^{-1}$ the scalar dissipation rate is entirely dominated by the mean behavior, reflecting the one dimensional nature of the plume at this point and the fact that mean concentration is a good representation of actual concentration at this time.

5. Conclusions

Quantifying mixing in heterogeneous porous media is a challenging affair as its accurate quantification requires knowledge of the full concentration field, specifically the gradients. Except at late asymptotic times when transverse dispersion has homogenized concentration in the vertical direction and

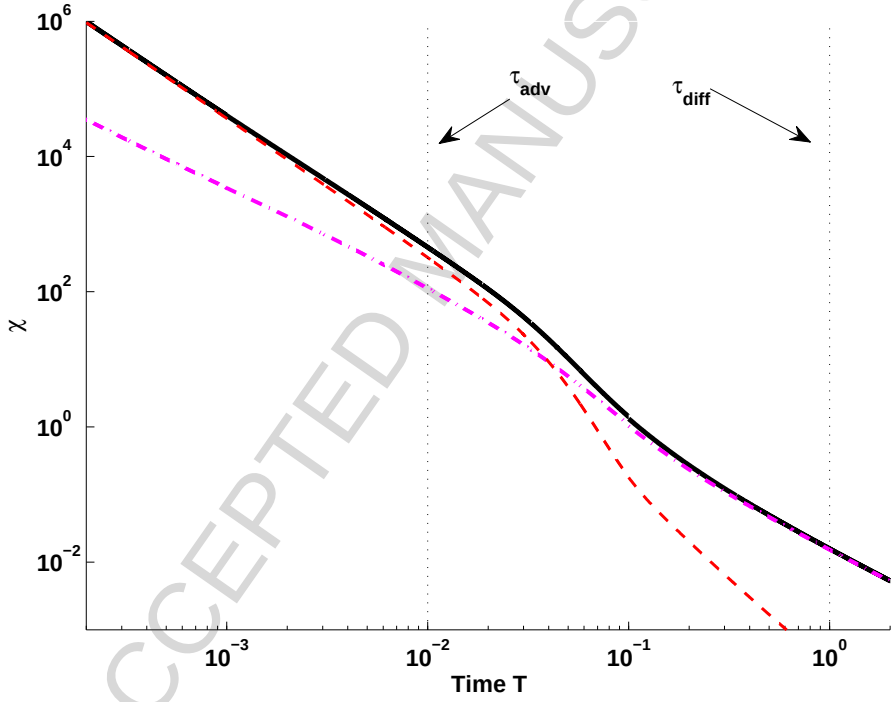

Figure 11: The scalar dissipation rate $\chi(t)$ against time for the point source initial condition in Poiseuille flow at various times. The black solid line represents the total contribution. The purple dash-dot line represents the contribution from the mean concentration field and the red dashed line that of the deviation concentration field. The two vertical dotted lines represent the advective and diffusive time scales for a Peclet number of 100.

the system is well represented by a Taylor dispersion coefficient, the mean concentration does not properly represent mixing.

Calculating the actual concentration distribution at early times is difficult, if not impossible, to solve as the governing equations for the mean and deviation concentrations are coupled and include nonlocal sources that make analytical approaches cumbersome. In this work we present an argument based on dominant balances using time and length scales (Valdés-Parada et al. (2009)), which indicates that regimes exist where certain terms that cause difficulty can be neglected or localized in such a manner as to allow approximate analytical estimates of mixing measures. In particular, as outlined in Appendix A, we neglect the local and nonlocal convective terms that contribute to the deviation concentration. This can be interpreted as either that vertical diffusive transport is much larger than the convective contribution or that the local and nonlocal convective terms balance one another. In this work we focus on the scalar dissipation rate as a measure of global mixing. We develop the analytical solutions for two typically studied initial conditions, a line source spanning the width of the domain and a point source. Since we decompose the concentration into a mean and deviation part and solve for each, we can also quantify the specific contribution of each to mixing as outlined in equations (25)-(28). Specifically, the contribution from the mean concentration represents spreading, while it is the combined contribution of mean and deviation that quantify mixing. This means that we can distinguish them.

By comparing the analytical predictions with numerical simulations for several flow fields we illustrate that this approximate analytical approach captures the true behavior of the scalar dissipation rate in a manner that a mean model can simply not do. In particular this work highlights the importance of the advective and dispersive timescales, which respectively are a measure of how long it takes for advective effects to play an influence on the system and how long it takes for dispersive effects to smooth out vertical gradients and return the system to an effective one-dimensional plume, as has been noted by several previous works (e.g. Dentz and Carrera (2007), Fiori and Dagan (2002), Zavala-Sanchez et al. (2009)). Before the advective time, considering local dispersion suffices to adequately capture mixing effects. For the case of the line source this means ignoring the deviation concentration effects, while for the point source it means ignoring the mean concentration effects. At these early times, mixing is entirely driven by local dispersion as spreading has not yet kicked in. At times later than the dispersive time scale

mixing is faithfully represented by the mean concentration and asymptotic Taylor dispersion coefficient, verifying that at these late time mixing and spreading are one and the same thing. However, between these two time scales both the mean and deviation concentration fields are of comparable order and neither can be neglected for the proper quantification of mixing. It is at these intermediate times that mixing and spreading effects, while intricately linked are not the same.

In the comparison with numerical results an interesting, although perhaps expected, feature emerges: the difference between the mean square concentration and the concentration fluctuation at intermediate times increases progressively as the flow fields become more heterogeneous (as quantified by the variance of the permeability field). This is because larger degrees of heterogeneity cause greater spreading and hence greater deviations from mean behavior. Interestingly, the Poiseuille flow case presents the largest relative difference between mean and total mixing. This is due to the longer wave length nature of this flow relative to others. In our solution this feature is captured by the low Fourier wavenumbers, which are larger for long wave length flows, which is what one might expect in a permeability field with a large correlation length. Again these reflect the greater degree of spreading induced by the longer wavelengths and that in turn influences mixing.

One of the principle motivations for evaluating mixing is to be able to quantify reactive transport, which for many reactions is driven by mixing. As illustrated in this work global mixing effects decay over multiple orders of magnitude over time (see figures 7 and 11). As such most of the critical reaction will take place at early times. This work illustrates that if the times of interest are in between the advective and dispersive timescales (which in practice is often the case) one must account for the fact that mixing and spreading effects will not be identical. Otherwise one is likely to miscalculate the actual reaction.

6. Acknowledgements

DB would like to thank the Spanish ministry of science for funding him and this project via the Juan de la Cierva program. This work was supported by the EU project MUSTANG and CIUDEN.

Appendix A. Averaging

We briefly outline the details related to the upscaling of the microscale balance equation; attention is focused on the length and time scale constraints that bound the validity of the resulting model. For full details on all of the assumptions and regimes of validity see Valdés-Parada et al. (2009).

Using the decomposition $c = \langle c \rangle + \widetilde{c}$ in (5) and subsequent averaging gives

$$\frac{\partial \langle c \rangle}{\partial t} + Pe \frac{\partial \langle c \rangle}{\partial x} = \frac{\partial^2 \langle c \rangle}{\partial x^2} - \frac{\partial \langle \widetilde{u}(y) \widetilde{c} \rangle}{\partial x}. \tag{A.1}$$

The initial and boundary conditions associated to the average concentration are given by (15).

Since no length or time scale constraints have been imposed, it can be assumed that Eq (A.1) is valid everywhere $\forall t > 0$. However, in its present form, Eq (A.1) is of little use since the deviation fields have not been computed at this point.

It is thus necessary to derive and solve the governing equations for $\widetilde{c}$. To this end the transport equation for the concentration deviations can be obtained by subtracting (A.1) from (1); this leads to

$$\frac{\partial \widetilde{c}}{\partial t} + u(y) \frac{\partial \widetilde{c}}{\partial x} + \widetilde{u}(y) \frac{\partial \langle c \rangle}{\partial x} = \left(\frac{\partial^2 \widetilde{c}}{\partial x^2} + \frac{\partial^2 \widetilde{c}}{\partial y^2} \right) + \frac{\partial \langle \widetilde{u}(y) \widetilde{c} \rangle}{\partial x} \tag{A.2}$$

where we have made use of the identity

$$u(y) \frac{\partial c}{\partial x} - Pe \frac{\partial \langle c \rangle}{\partial x} = \widetilde{u}(y) \frac{\partial \langle c \rangle}{\partial x} + u(y) \frac{\partial \widetilde{c}}{\partial x} \tag{A.3}$$

Recall that $\langle u \rangle = Pe$.

In its present form, Eq (A.2) contains a non-local convective term. This term makes it necessary to account for the fields of $\widetilde{c}$ at all times in order to solve Eq (A.2), thus leading to iterative solutions. We perform an order of magnitude analysis of this nonlocal convective term in Eq (A.2), which leads to

$$\frac{\partial \langle \widetilde{u}(y) \widetilde{c} \rangle}{\partial x} = \mathbf{O} \left(\frac{Pe \widetilde{c}}{L_x} \right) \tag{A.4}$$

where L_x denotes the characteristic length associated to the variations of $\widetilde{c}$ in the x-direction. Indeed, during the unsteady stages of transport L_x is a function of time as discussed in detail by Valdés-Parada et al. (2009). In

addition, in Eq (A.4) we have used the estimate $\widetilde{u} = \mathbf{O}(Pe)$, which is justified by (i) the non-slip condition of the fluid velocity at the walls of the system (Whitaker (1999)) for Poiseille flow and (ii) the non-negativity of $u(y)$ and finite variance of K for the stratified medium case.

Furthermore, an order of magnitude analysis of the diffusive term in the y-direction in Eq (A.2) shows that

$$\frac{\partial^2 \widetilde{c}}{\partial y^2} = \mathbf{O}\left(\widetilde{c}\right) \tag{A.5}$$

In writing this estimate, we have restricted the analysis to *sufficiently large* time periods so that the characteristic length associated to the transport in the y-direction can be taken to be the width of the flow space (which is 1 in non-dimensional terms). This is usually the case during the preasymptotic time stage (i.e., after the early time stage, see Valdés-Parada et al. (2009)). On the basis of the estimates in Eqs (A.4) and (A.5), we note that whenever the constraint

$$\frac{Pe}{L_x} \ll 1 \tag{A.6}$$

is satisfied, it can be concluded that

$$\frac{\partial \left\langle \widetilde{u}(y)\widetilde{c} \right\rangle}{\partial x} \ll \frac{\partial^2 \widetilde{c}}{\partial y^2}. \tag{A.7}$$

Moreover, a similar analysis shows that the local and non-local convection terms in Eq (A.2) are of the same order of magnitude, i.e,

$$u(y)\frac{\partial \widetilde{c}}{\partial x} = \mathbf{O}\left(\frac{\partial \left\langle \widetilde{u}(y)\widetilde{c} \right\rangle}{\partial x}\right) \tag{A.8}$$

Therefore, on the basis of the constraint in (A.6), it can also be deduced that

$$u(y)\frac{\partial \widetilde{c}}{\partial x} \ll \frac{\partial^2 \widetilde{c}}{\partial y^2}. \tag{A.9}$$

This condition and that in A.7 suggests that vertical diffusive processes are much stronger than horizontal advection (both local and nonlocal) ones. Under these conditions, (A.2) simplifies to

$$\frac{\partial \widetilde{c}}{\partial t} - \left(\frac{\partial^2 \widetilde{c}}{\partial x^2} + \frac{\partial^2 \widetilde{c}}{\partial y^2}\right) = \widetilde{u}(y)\frac{\partial \langle c \rangle}{\partial x} \tag{A.10}$$

As mentioned above, this equation arises when vertical diffusive processes in $\widetilde{c}$ dominate horizontal convective contributions. Alternatively, one can think of it as arising when there is a balance between the local $(u(y)\frac{\partial \widetilde{c}}{\partial x})$ and nonlocal $(\frac{\partial \langle \widetilde{u}(y)\widetilde{c}\rangle}{\partial x})$ convective terms in (A.2). The initial-boundary conditions for (A.10)are given by (17).

Notice that the concentration deviation fields are driven by the initial condition and by the convective source. Since we have neglected the convective terms in (A.10), it can be reasoned that the concentration deviations account for the unsteady microscale mixing in the x and y directions. This process is driven, in general, by the displacements of the convective source in the x-direction.

Our next step in the analysis is to use standard Green's functions analysis, to obtain the formal solution for $\widetilde{c}$. This yields

$$\widetilde{c}(x,y,t) = \int_0^1 \int_{-\infty}^{\infty} \widetilde{F}(\xi,\eta) G(x-\xi,y,t|\eta) d\xi d\eta - \int_0^t \int_0^l \int_{-\infty}^{\infty} \widetilde{u}(\eta) \frac{\partial \langle c\rangle(\xi,\tau)}{\partial \xi} G(x-\xi,y,t-\tau|\eta) d\xi d\eta d\tau. \quad \text{(A.11)}$$

The Green's function is given by

$$G(x,y,t|\eta) = G_y(y,t|\eta) \frac{\exp\left(-\frac{x^2}{4t}\right)}{\sqrt{4\pi t}} \quad \text{(A.12)}$$

where, the Green's function in the y direction is given by (e.g. Carslaw and Jaeger, 1959)

$$G_y(y,t|\eta) = 1 + 2\sum_{n=1}^{\infty} \cos(n\pi y)\cos(n\pi\eta)\exp\left(-n^2\pi^2 t\right) \quad \text{(A.13)}$$

Substituting (A.11) into (A.2) leads to a spatio-temporally non-local average equation, see also (e.g. Neuman, 1993; Morales-Casique et al., 2006) for similar analyses in a divergence-free random flow field.

Here we localize (A.11), which gives (19), where $b_0(x,t)$ and $b_1(x,y,t)$ are

given by

$$b_0(x,y,t) = \int_0^1 \int_{-\infty}^{=\infty} \widetilde{F}(\xi,\eta) G(x-\xi,y,t|\eta) d\xi d\eta \tag{A.14}$$

$$b_1(y,t) = -\int_0^t \int_0^1 \widetilde{u}(\eta) G_y(y,t-\tau|\eta) d\eta d\tau \tag{A.15}$$

Valdés-Parada et al. (2009) discuss the conditions under which (A.11) can be localized.

Our final step in the analysis is to close the average model by substituting the closure problem solution (19) into (A.1). After some rearrangement, the resulting expression can be written as

$$\frac{\partial \langle c \rangle}{\partial t} + Pe \frac{\partial \langle c \rangle}{\partial x} = D^a(t) \frac{\partial^2 \langle c \rangle}{\partial x^2} + \phi(x,t) \tag{A.16}$$

where we have introduced the time-dependent Taylor dispersion coefficient

$$D^a(t) = 1 - \langle \widetilde{u}(y) b_1(y,t) \rangle \tag{A.17}$$

and the memory function $\phi(x,t)$ that accounts for the influence of the initial condition

$$\phi(x,t) = -\left\langle \widetilde{u}(y) \frac{\partial b_0(x,y,t)}{\partial x} \right\rangle. \tag{A.18}$$

The solution for $\langle c \rangle$ is given by (18), where $d_0(x,t)$ and $d_1(x,t)$ are given by

$$d_0(x,t) = \int_{-\infty}^{\infty} g(x-\xi,t|0) \langle F \rangle(\xi) \mathrm{d}\xi \tag{A.19}$$

$$d_1(x,t) = \int_0^t \int_{-\infty}^{\infty} g(x-\xi,t|\tau) \phi(\xi,\tau) \mathrm{d}\xi \mathrm{d}\tau. \tag{A.20}$$

The Green's function $g(x,t|\tau)$ is given by (32) for $t_0 = \tau$.

Appendix B. Random Walk Simulations

The transport problem is solved numerically by random walk simulations based on the Langevin equation. In discrete time, the equation of motion of the nth solute particle reads as

$$\begin{aligned} x(t+\Delta t|\mathbf{x}') &= x(t,\mathbf{x}') + u\left[\mathbf{x}(t|\mathbf{x}')\right]\Delta t + \sqrt{2D\Delta t}\eta_1 \\ y(t+\Delta t|\mathbf{y}') &= y(t,\mathbf{y}') + \sqrt{2D\Delta t}\eta_2 \end{aligned} \tag{B.1}$$

The η_i $(i = 1, \ldots, d)$ are independently distributed Gaussian random variables with zero mean and variance one. The impermeable channel walls are modeled as reflecting boundaries.

The simulations presented release 1×10^6 particles from each initial position. The line source is represented by individual particles equally distributed across the width of the channel at $x = 0$.

References

Aris, R., 1956. On the dispersion of a solute in a fluid flowing through a tube. Proc Roy Soc A 235, 67.

Battiato, I., Tartakovsky, A., Tartakovsky, D., Scheibe, T., 2009. On breakdown of macroscopic models of reactive transport in porous media. Advances in Water Resources In Press.

Bear, J., 1972. Dynamics of fluids in porous media. Elsevier, New York.

Berentsen, C. W. J., Verlaan, M. L., van Kruijsdijk, C. P. J. W., 2005. Upscaling and reversibility of taylor dispersion in heterogeneous porous media. Phys. Rev. E 71, 046308.

Berentsen C.W.J. and C.P.J.W. van Kruijsdijk 2008 Relaxation and reversibility of extended Taylor dispersion from a MarkovianLagrangian point of view . Advances in Water Resources, Volume 31, P 609-629

Bolster, D., Barahona, M., Dentz, M., Fernandez-Garcia, D., Sanchez-Vila, X., Trinchero, P., Valhondo, C., Tartakovsky2, D. M., 2009a. Probabilistic risk analysis of groundwater remediation strategies. Water Resources Research 45, W06413, doi:10.1029/2008WR007551.

Bolster, D., Dentz, M., Carrera, J., 2009b. Effective two-phase flow in heterogeneous media under temporal pressure fluctuations. Water Resour. Res 45, W05408, doi:10.1029/2008WR007460.

Bolster, D., Dentz, M., LeBorgne, T., 2009c. Solute dispersion in channels with periodically varying apertures. Physics of Fluids 21, 056601 DOI:10.1063/1.3131982.

Bouchaud, J. P., Georges, A., 1990. Anomalous diffusion in disordered media: Statistical mechanisms, models and physical applications. Phys. Rep. 195 (4,5), 127–293.

Bouchaud, J. P., Georges, A., Koplik, J., Provata, A., Redner, S., 1990. Superdiffusion in random velocity fields. Phys. Rev. Lett. 64 (21), 2503–2506.

Brenner, H., Edwards, D., 1993. Macrotransport Processes. Butterworth-Heinemann, Woburn, Massachusetts, USA.

Camacho, J., 1993. Purely global model for Taylor dispersion. Phys. Rev. E 48 (1), 310–320.

Carslaw, H. S., Jaeger, J. C., 1959. Conduction of Heat in Solids. Oxford University Press, New York.

Cvetkovic, V., Shapiro, A., 1989. Solute advection in stratified formations. Water Resour. Res. 25, 1283–1290.

Dagan, G., 1988. Time-dependent macrodispersion for solute transport in anisotropic heterogeneous aquifers. Water Resources Research 24 (9), 1491–1500.

Dagan, G., 1990. Transport in heterogeneous porous formations: Spatial moments, ergodicity and effective dispersion. Water Resources Research 26, 14281–1290.

De Simoni, M., Carrera, J., Sánchez-Vila, X., Guadagnini, A., 2005. A procedure for the solution of multicomponent reactive transport problems. Water Resour. Res. 41, 2005WR004056.

Dentz, M., Carrera, J., 2007. Mixing and spreading in stratified flow. Phys Fluids 19, 017107.

Dentz, M., Carrera, J., Bolster, D., LeBorgne, T., 2009. Multipoint concentration statistics for transport in stratified random velocity fields. Physical Review E 8, 036306.

Dentz, M., Kinzelbach, H., Attinger, S., Kinzelbach, W., 2002. Temporal behavior of a solute cloud in a heterogeneous porous medium 3. numerical simulations, water resour. res. Water Resour. Res. 38 (7), 1118.

Dentz, M., LeBorgne, T., Carrera, J., 2008. Effective transport in random shear flows. Phys Rev E 77, 020101.

Dreuzy, J., Erhel, A. B. J., 2007. Asymptotic dispersion in 2d heterogeneous porous media determined by parallel numerical simulations. Water Resour. Res 43, W10439.

Fernandez-Garcia, D., Sanchez-Vila, X., Guadagnini, A., 2008. Reaction rates and effective parameters in stratified aquifers. Advances in Water Resources, Volume 31, Issue 10, October 2008, Pages 1364-1376 31, 1364–1376.

Fiori, A., Dagan, G., 2002. Transport of a passive scalar in a stratified porous medium. Transp. Porous Media 47, 81–98.

Gelhar, L.J., Gutjahr, A.L. and Naff, R.L.: 1979, Stochastic analysis of macrodispersion in a stratified aquifer, Water Resour. Res. 15, 1387-1397

Gelhar, L. W., Axness, C. L., 1983. Three-dimensional stochastic analysis of macrodispersion in aquifers. Water Resour. Res. 19 (1), 161–180.

Gill, W. N., Sankarasubramanian, R., 1970. Exact analysis of unsteady convective diffusion. Proc Roy Soc A 316, 341.

Güven, O., Molz, F., Melville, J. G., 1984. An analysis of macrodispersion in a stratified aquifer. Water Resour. Res. 20 (10), 1337–1353.

Kapoor, V., Anmala, J., 1998. Lower bounds on scalar dissipation in bounded rectilinear flows. Flow, Turbulence and Combustion 60, 125–156.

Kapoor, V., Gelhar, L. W., 1994a. Transport in three-dimensionally heterogeneous aquifers, 1, Dynamics of concentration uctuations. Water Resour. Res 30, 17751778.

Kapoor, V., Gelhar, L. W., 1994b. Transport in three-dimensionally heterogeneous aquifers, 2, Predictions and observations of concentration uctuations. Water Resour. Res 30, 1789 1801.

Kapoor, V., Kitanidis, P., 1998. Concentration fluctuations and dilution in aquifers. Water Resour. Res 34, 1191–1193.

Kapoor, V., Kitanidis, P. K., 1997. Advection-diffusion in spatially random flows: formulation for the concentration covariance ., 11(5), 397-422, 1997. Stoch. Hydrol. Hydraul 11, 297–422.

Kitanidis, P. K., 1994. The concept of the dilution index. Water Resour. Res. 30, 2011–1026.

Latini, M., Bernoff, A. J., 2001. Transient anomalous diffusion in poiseuille flow. J. Fluid. Mech. 441, 339.

LeBorgne, T., Dentz, M., Carrera, J., 2008a. Lagrangian statistical model for transport in highly heterogeneous velocity fields. Physical Review Letters 101, 090601.

LeBorgne, T., Dentz, M., Carrera, J., 2008b. Spatial markov processes for modeling lagrangian particle dynamics in heterogeneous porous media. Physical Review E 78, 026309.

Lighthill, M. J., 1966. Initial development of diffusion in Poiseuille flow. J. Inst. Maths Appl. 97, 2001.

Lunati, I., Attinger, S., Kinzelbach, W., 2002. Macrodispersivity for transport in arbitrary nonuniform flow fields: Asymptotic and preasymptotic results. Water Resour. Res 38(10), 1187, doi:10.1029/2001WR001203.

Marle, C., Simandoux, P., Pacsirsky, J., Gaulier, C.: 1967, Etude du deplacement de fludes miscibles en milieu poreux stratifie, Rev. Inst. Fr. Pet. 22, 272-294.

Mercado, A.: 1967, The Spreading Pattern of Injected Waters in a Permeability Stratified Aquifer, IAHS Publ. No. 72, 23-36.

Matheron, G., de Marsily, G., 1980. Is transport in porous media always diffusive? a counterexample. Water Resources Res 16, 901.

Mercer, G. N., Roberts, A. J., 1990. A center manifold description of contaminant dispersion in channels with varying flow properties. SIAM J. Appl. Math. 50, 1547–1565.

Morales-Casique, E., Neuman, S. P., Guadagnini, A., 2006. Non-local and localized analyses of non-reactive solute transport in bounded randomly heterogeneous porous media: Theoretical framework. Adv. Water Res. in press.

Neuman, S. P., 1993. Eulerian-lagrangian theory of transport in space-time nonstationary velocity fields: Exact nonlocal formalism by conditional moments and weak approximation. Water Resour. Res. 29 (3), 633–645.

Neuweiler, I., Attinger, S., Kinzelbach, W., King, P., 2003. Large scale mixing for immiscible displacement in heterogeneous porous media. Transport in Porous Media 51, 287–314.

Pope, S., 2000. Turbulent Flows. Cambridge University Press.

Porter, M., Valdés-Parada, F., Wood, B., 2008. Direct numerical simulations of transient dispersion, AGU Fall Meeting 2008.

Redner, S., 1990. Superdiffusion in random velocity fields. Physica A 168, 551–560.

Taylor, G. I., 1953. Dispersion of soluble matter in solvent flowing slowly through a tube. Proc. Roy. Soc. A 219, 186.

Valdés-Parada, F., Porter, M., Wood, B., 2009. Time scales for Taylor dispersion. Journal of Fluid Mechanics Under Review.

Whitaker, S., 1999. The method of volume averaging. Kluwer Academic Publishers.

Young, W. R., Jones, S., 1991. Shear dispersion. Phys. Fluids A 3 (5), 1087–1101.

Zavala-Sanchez, V., Dentz, M., Sanchez-Vila, X., 2009. Characterization of mixing and spreading in a bounded stratified medium. Adv. Water Resour. 32 (5), 635–648.

Zumofen, G., Klafter, J., Blumen, A., 1990. Enhanced diffusion in random velocity fields. Phys. Rev. A 42, 4601–4608.